Dressed skeleton expansion in (1+1)-dimensional field-theory models

Hung Jung Lu
Stanford Linear Accelerator Center, Stanford University, Stanford, California 94309
(Received 8 July 1991; revised manuscript received 7 October 1991)

We discuss the implementation of the dressed skeleton expansion (DSE) and analyze various features of this perturbative calculational method in simple field-theory models in 1+1 dimensions. In particular, we investigate issues concerning loop skeleton diagrams, renormalization in the massive case, and the usage of the DSE for vertices involving matrix strucures.

PACS number(s): 11.10.Gh

I. INTRODUCTION

In a previous paper [1], we pointed out that the dressed skeleton expansion (DSE) offers a calculational method in perturbative quantum field theories without the scale-ambiguity problem. In particular, we illustrated the usage of the method for ϕ^3 theory in six dimensions. The basic motivation in choosing this theory resides in its resemblance to quantum chromodynamics (QCD) in the aspects of both being renormalizable theories and presenting asymptotic freedom. However, the high dimensionality of the theory hampered the discussion of higher-order skeleton graphs.

In this paper we study the application of the DSE to field-theory models in 1+1 dimensions. Our purpose is to analyze and discuss the various features and technical details for the implementation of the DSE method by using simple models as the testing ground. It is not our goal to obtain new results in these simple field-theory models, for there exists abundant literature on the subject [2,3].

This paper is organized in the following sections: In Sec. II, we discuss the general scale-setting problem in quantum field theories, and present the DSE as a scale-ambiguity-free calculational method. In Sec. III we give an overview of the general skeleton expansion. In Sec. IV we describe the details of the DSE. We also point out there its relationship with the Brodsky-Lepage-Mackenzie (BLM) [4] scale-setting method in QED. In Sec. V we apply the DSE method to the massless Gross-Neveu model in leading $1/N$ expansion, and show that the DSE leads to an exact four-fermion vertex function, regardless of whether we choose to dress up the charged two-point function or the three-point function. In Sec. VI we apply the DSE method to the $N=2$ Gross-Neveu model without the $1/N$ expansion. Here we offer an explicit example of a nontrivial loop skeleton diagram, showing that it indeed can be done and yields a finite result, despite the singularity of the coupling vertex at the Landau pole. We give an argument for the insensitivity of loop skeleton diagrams to the infrared behavior of vertex functions. In Sec. VII we apply the DSE method to the super-renormalizable massive Yukawa model in 1+1 dimensions. This is an example where the vertex function has a nontrivial matrix structure, and special attention is required to select a coupling function that ensures the continuity of the off-shell to on-shell transition. Also, in this example, we show how to isolate the mass renormalization from particle propagators and absorb all renormalization effects of two-point functions into effective wave-function renormalization constants. Finally, in Sec. VIII, we make some comments and summarize the main conclusions.

II. SCALE-SETTING PROBLEM AND THE DRESSED SKELETON EXPANSION

Perturbative calculations in quantum field theories are usually expressed as power series in a fixed coupling constant. At high squared momentum transfer, the fixed coupling constant must be replaced by a running coupling constant. This procedure is usually referred to as the renormalization-group-improved perturbation, which leads to the absorption of the large logarithmic terms into the running coupling constant. In simple words, given a truncated series of a physical quantity expanded in powers of a coupling constant in a given scheme,

$$R_n=\alpha^s(\mu)[r_0+r_1(\mu)\alpha(\mu)+\cdots+r_n(\mu)\alpha^n(\mu)]\ , \tag{1}$$

the coupling μ must be chosen appropriately for the perturbative series to be useful. The unknown dependence of the truncated series on μ is commonly referred to as the coupling-scale-ambiguity problem. There is also another source of ambiguity in the perturbative expansion arising from the freedom in the choice of the renormalization scheme. However, we have argued in our previous paper [1] that the scale ambiguity is a more fundamental problem than the corresponding scheme ambiguity in the sense that, if one is able to solve the general scale-setting problem, then there is no ambiguity in how to implement different schemes.

Several methods have been proposed to solve the coupling-scale ambiguity. Among them we shall mention the following.

(1) Fastest apparent convergence (FAC) [5,6]. The idea behind FAC is that one should choose the coupling scale that makes the series look like most convergent. Frequently it is defined as the condition of a vanishing second-order term (i.e., next to tree level) coefficient. A related topic is the "effective charge" [5] or the

"renormalization-scheme-invariant" (RSI) [7] method, where one effectively requires all higher-order coefficients to be zero.

(2) Principle of minimal sensitivity (PMS) [6]. We shall define it here as the choice of the coupling scale at the stationary point of the truncated series:

$$\left.\frac{dR}{d\mu}\right|_{\mu}=0 \ . \tag{2}$$

The PMS method also aims toward the choice of a renormalization scheme, and beyond two-loop order this method requires the variation of scheme parameters in addition to the coupling scale.

(3) Brodsky-Lepage-MacKenzie [4]. This method is inspired from QED. The philosophy is to absorb all fermionic vacuum-polarization effects into the running coupling constant. In one-loop-order massless QCD it is operationally equivalent to the condition of a vanishing coefficient of the n_f (number of light fermions) term. Therefore, the BLM results are formally invariant under the change of number of light favors:

$$\frac{\partial R}{\partial n_f}(\alpha(\mu),n_f)=0 \ . \tag{3}$$

The usual impression is that, as long as the coupling scale μ^2 is chosen near the typical scale Q^2 of a given process, the perturbation series would give a reasonable result. We should notice, however, that, due to dimensional transmutation (i.e., the presence of $\Lambda_{\rm QCD}$), the correct scale in some cases might not be proportional to Q^2 but rather to some other power of it, or even in a more complicated way. So the naive form of assigning a coupling scale to typical physical scales runs the danger of being too simplistic. Also, for processes involving many scales, in general, it is not clear how a "typical scale" can be defined.

For multiscale processes, the conventional way of assigning a uniform coupling throughout all vertices becomes questionable. Consider, for instance, the exclusive process $e^+e^-\to\mu^+\mu^-\gamma$ (Fig. 1). In QED the vertices a and b should have a coupling strength $\sim\alpha^{1/2}(Q^2)$ whereas the vertex involving the radiated photon should have a strength $\sim\alpha^{1/2}(0)=1/\sqrt{137}$.

This observation and the existing controversy on the various scale-setting procedures prompt us to explore the dressed skeleton expansion instead of the conventional power-series expansion. The ingredients of a skeleton-type calculation are the following: (1) The basic vertex functions are calculated by using renormalization-group equations [8]; (2) any other Green's function is expanded in skeleton graphs of the basic vertices.

More details on DSE are discussed in the next two sections, but let us point out here some of its features. One property of this calculational procedure is that it is automatically scale-ambiguity-free because there is no exogenous coupling constant. In fact, this automatic scale-setting feature in QED is the basis of the BLM scale-setting method. The DSE effectively extends BLM's method in QED to other field theories. Let us stress here that, unlike conventional perturbative methods, DSE is

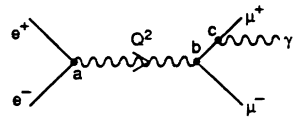

FIG. 1. A typical QED process, where the coupling strength at vertices a and b is expected to be stronger than the coupling strength at c.

not a power-series expansion in a coupling constant: it is a functional expansion in term of a dressed vertex function. In DSE there are no coupling constants. In general, the results in DSE calculations are expressed directly in terms of functions that involve a scale analogous to $\Lambda_{\rm QCD}$. This should not come as a surprise. In fact, the concept of a coupling constant is also lost in conventional perturbation theory with the scale-fixing procedure. After scale fixing, the results in perturbative QCD are directly expressed in term of $\Lambda_{\rm QCD}$. In this sense, the coupling constant merely serves as an intermediate device and is discarded after scale fixing. Another argument in favor of the dressed skeleton expansion is that many of the renormalon-type contributions [9,10] are automatically resummed into the full propagators and vertex functions; therefore, there is good reason to expect higher-order skeleton results to have better convergence properties than the conventional power-series expansion.

III. WHAT ARE SKELETONS?

The skeleton expansion is a particular way of organizing Feynman diagrams that are equivalent up to self-energy and vertex insertions. The original idea of the skeleton expansion can be traced back to Dyson [11] in the late 1940s. In the development of quantum field theories, the skeleton expansion has been a common technique in the proof of perturbative renormalizability [12–14]. The skeleton analysis has also been studied with the hope that some nonperturbative features can be revealed by solving the set of coupled integral equations [18]. However, the Bogoliubov-Parasiuk-Hepp-Zimmermann (BPHZ) [15] formalism based on Bogoliubov's R operation [15,16] and Zimmermann's forest formula [15,17] has proven to be much more effective in tackling questions on perturbative renormalizability, and hence has become the standard approach taken by most modern textbooks [20]. Although the skeleton expansion was once widely known to the community, an increasing general unfamiliarity with it makes us believe that a brief review of its basic ideas would be helpful to the reader.

Skeleton graphs represent Feynman diagrams that differ only by vertex and self-energy insertions. To fix the idea, let us consider Feynman diagrams in ϕ_6^3 theory [21]. Take, for instance, the graph depicted in Fig. 2 (adapted from Bjorken and Drell [13]). To obtain the skeleton graph of this particular Feynman diagram, we draw a box around each vertex or self-energy insertion. We observe that the boxes are either disjoint or nested, with one exception: within self-energy insertions the boxes may overlap. The nonoverlapping property is actually true for all graphs: the boxes enclosing vertex and self-energy

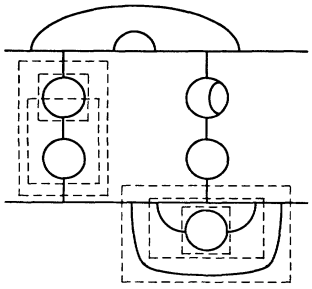

FIG. 2. An example of Feyman diagram where we have boxed some of the vertex and self-energy insertions.

insertions may always be drawn in such a way that they never overlap, except for a vertex insertion within self-energy parts (see Ref. [13] for proof).

As a consequence of this nonoverlapping property, we may associate in a unique way with each graph G another graph called the skeleton graph of G. For instance, Fig. 3 corresponds to the skeleton graph of Fig. 2.

In Fig. 4 we give some more examples to clarify the concept of skeleton graphs. Notice that by definition skeleton graphs are those that cannot be further reduced by removing vertex or self-energy insertions. Thus, Fig. 4(b) is a skeleton graph, while Figs. 4(a) and 4(c) are not skeleton graphs.

Because of the nonoverlapping property, we can generate the complete set of Feynman diagrams corresponding to a particular scattering amplitude (i.e., any connected and amputated n-point Green's function with $n > 3$) by (1) first drawing all the possible skeleton graphs with n external legs, then (2) replacing the propagators in the skeleton graphs by full propagators and the vertices by full vertex functions.

As an example, the two-body scattering amplitude in ϕ_6^3 theory will contain the skeleton graphs shown in Fig. 5. The full propagator and full vertex graphs are shown in Fig. 6. From the nonoverlapping property, we can convince ourselves that all Feynman diagrams of this scattering amplitude are effectively contained once and only once in the skeleton expansion.

The basic idea behind the standard approach of renormalization by employing skeleton expansion analysis lies in the following.

(1) Let $Z_{\rm OS}$ be the on-shell wave-function renormalization constant, that is, the residue of the full propagator at the physical mass pole. Define the renormalized propagator by dividing the full propagator by $Z_{\rm OS}$ (see Fig. 7).

(2) Define the renormalized vertex function by multiplying the full vertex function by $Z_{\rm OS}^{3/2}$ (see Fig. 7).

(3) According to the Lehmann-Symanzik-Zimmermann (LSZ) [19] reduction formula, we also multiply the overall amplitude by $Z_{\rm OS}^{n/2}$ in order to obtain the renormalized scattering amplitude, where n is the number of external legs.

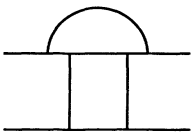

FIG. 3. Skeleton graph of Fig. 2.

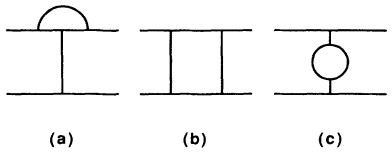

FIG. 4. (b) is a skeleton graph, whereas (a) and (c) are not skeleton graphs.

(4) As a consequence, renormalized scattering amplitudes can be written in terms of renormalized skeleton graphs consisting only of renormalized propagators and renormalized vertex functions. This is shown schematically in Fig. 7 for the two-particle scattering amplitude.

It is a rather involved task to rigorously prove that skeleton expansion indeed leads to a finite theory for all renormalized Green's functions. We shall assume in the following that the set of skeleton graphs to a given order in the number of vertices yields a finite result. The proof of this statement in QED is given by Bjorken and Drell [13], and in ϕ_4^4 theory by Zinn-Justin [14].

IV. DRESSED SKELETON EXPANSION

The dressed skeleton expansion [1] is an adaptation of the standard skeleton expansion. Two essential modifications are introduced.

(1) Local effective wave-function renormalizations. Instead of a unique, on-shell wave-function renormalization constant $Z_{\rm OS}$, there is a diagrammatically local effective wave-function renormalization "constant" $Z(p^2)$ per each full propagator. The idea is to absorb all self-energy renormalization effects into effective wave-function renormalization constants. More precisely, full, unrenormalized propagators are defined to be

$$i\Delta(p^2)=\frac{iZ(p^2)}{p^2-m_{\rm ph}^2}\ , \tag{4}$$

where $m_{\rm ph}$ is the physical mass. The effective wave-function renormalization constant coming from a particular full propagator is used to renormalize the vertices immediately adjacent to it. That is, at each vertex, the full, unrenormalized vertex function is to be multiplied by

$$Z^{1/2}(p^2)Z^{1/2}(q^2)Z^{1/2}(r^2) \tag{5}$$

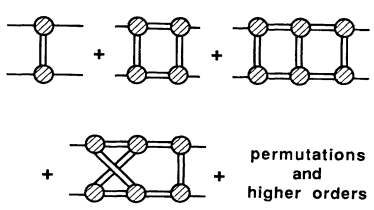

FIG. 5. Skeleton expansion for the two-particle scattering amplitude in ϕ^3 theory.

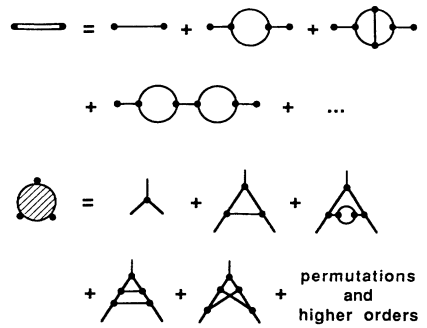

FIG. 6. Full propagator and full vertex functions in the ϕ^3 theory.

p^2, q^2, and r^2 being the squared momentum of the three legs attached to the particular vertex function (see Fig. 8).

Observe that this prescription is consistent with the LSZ prescription of multiplying $Z_{\rm OS}^{1/2}$ (the on-shell wave-function renormalization constant) per each external leg. Effectively, for all external legs we have $Z^{1/2}(p^2=m_{\rm ph}^2)=Z_{\rm OS}^{1/2}$; thus, all vertices attached to external legs are (and hence the overall amplitude, too, is) multiplied by the correct power of $Z_{\rm OS}^{1/2}$.

The two-body scattering amplitude in DSE to one-loop skeleton order consists of the skeleton graphs given in Fig. 9. Notice now that, in order to compute the skeleton graphs in Fig. 9, we have to know only one single function: the DS (dressed skeleton) vertex function. Obviously this holds true for any n-point ($n>3$) connected and amputated Green's functions: once known the DS vertex function, all higher-order Green's functions can be expressed as functional expansions in terms of the DS vertex function, being the functional expansion graphically represented by the DSE graphs. This is, in fact, why DSE is scale-ambiguity-free. In DSE there is no coupling constant and, thus, no undetermined coupling scale. Instead of the coupling constant we have a DS vertex function, and the (known) momenta flowing into it are effectively replacing the role of the (unknown) coupling scale of the conventional power-series expansion.

(2) Vertex function through a renormalization-group

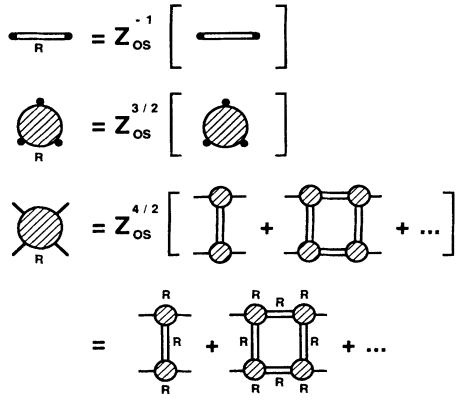

FIG. 7. Renormalized skeleton expansion in the ϕ^3 theory for the two-particle scattering amplitude.

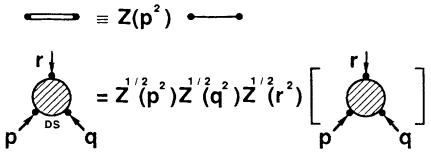

FIG. 8. Propagator and vertex function renormalization in DSE.

equation. The vertex function can be obtained by multivariable renormalization-group equation or other suitable techniques.

The multimomentum renormalization-group equation is an intuitive generalization of the usual β-function formalism. If the perturbative DS vertex function $\lambda_{\rm DS}(k_1,k_2,k_3)$ in terms of the bare coupling constant is

$$\lambda_{\rm DS}(k_1,k_2,k_3)=\lambda_0+\lambda_0^3 f_1(k_1,k_2,k_3)+\lambda_0^5 f_2(k_1,k_2,k_3)+\cdots , \tag{6}$$

where the coefficient functions f_i contain both divergent and finite parts, then we can obtain the multimomentum renormalization-group equation by (1) taking the derivative of Eq. (6) with respect to the external momenta,

$$\frac{\partial\lambda_{\rm DS}}{\partial k_i^\mu}=\lambda_0^3\frac{\partial f_1}{\partial k_i^\mu}+\lambda_0^5\frac{\partial f_2}{\partial k_i^\mu}+\cdots , \tag{7}$$

(2) formally inverting the Eq. (6) to expand λ_0 in power series of $\lambda_{\rm DS}$,

$$\lambda_0=\lambda_{\rm DS}-\lambda_{\rm DS}^3 f_1-\lambda_{\rm DS}^5(f_2-3f_1^2)-\cdots , \tag{8}$$

and (3) replacing Eq. (8) into the right-hand side of Eq. (7),

$$\frac{\partial\lambda_{\rm DS}}{\partial k_i^\mu}=\lambda_{\rm DS}^3\frac{\partial f_1}{\partial k_i^\mu}+\lambda_{\rm DS}^5\left[\frac{\partial f_2}{\partial k_i^\mu}-3f_1\frac{\partial f_1}{\partial k_i^\mu}\right]+\cdots \equiv\lambda_{\rm DS}^3\beta_1(\{k_i\})+\lambda_{\rm DS}^5\beta_2(\{k_i\})+\cdots . \tag{9}$$

When the underlying theory is renormalizable, all the coefficient functions $\beta_i(\{k_i\})$ of the multimomentum β function should be finite. The DS vertex function $\lambda_{\rm DS}$ can be obtained by solving this equation with the specification of an integration constant (usually in the guise of a quantity analogous to $\Lambda_{\rm QCD}$).

To one-loop order, however, the renormalization-group equation is equivalent to the well-known trick of eliminating the bare coupling constant through the introduction of an integration constant. That is, if

$$\lambda_{\rm DS}(\{k_i\})=\lambda_0+\lambda_0^3\left[\frac{c}{\epsilon}+f(\{k_i\})\right]+O(\lambda_0^5) , \tag{10}$$

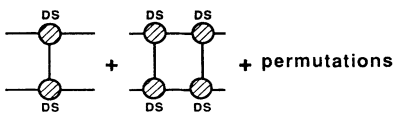

FIG. 9. DSE graphs for the two-particle scattering amplitude in ϕ^3 theory.

where the divergent part in the order-λ_0^3 term is taken care of through the $1/\epsilon$ pole term, then formally

$$\frac{1}{\lambda_{\rm DS}^2(\{k_i\})}=\frac{1}{\lambda_0^2}-\frac{2c}{\epsilon}-2f(\{k_i\})+O(\lambda_0^2)\ . \tag{11}$$

This last equation is valid for any set of values of $\{k_i\}$; therefore, we also have

$$\frac{1}{\lambda_{\rm DS}^2(\{k_i'\})}=\frac{1}{\lambda_0^2}-\frac{2c}{\epsilon}-2f(\{k_i'\})+O(\lambda_0^2)\ . \tag{12}$$

Taking the difference between these last two equations and neglecting higher-order terms, we obtain

$$\lambda_{\rm DS}^2(\{k_i\})=\frac{1}{C-2f(\{k_i\})}\ , \tag{13}$$

where $C=2f(\{k_i'\})+1/\lambda_{\rm DS}^2(\{k_i'\})$ is effectively an integration constant.

The exact formula for the vertex function to one-loop order in ϕ_6^3 theory is somewhat complicated, but in the small-mass limit, and when some of the legs are on shell, the corresponding simplified expressions can be obtained [1].

We notice that the expansion order in DSE is twofold, we have to specify (1) the number of vertices that is used in expanding a general scattering amplitude in term of the DS vertex function, and (2) the number of terms that is used to compute the renormalization-group equation for the DS vertex function. This actually also happens in the conventional method of perturbative calculations: the results in perturbative QCD also contain two expansion orders, one corresponding to the order of the result itself in terms of the running coupling constant, and the other one corresponding to the order that is used in obtaining the running coupling constant through the β-function formalism. In principle, there is no requirement in matching one order with another, but, in practice, these two orders are often kept the same.

The case of QED. In QED, because of the Ward identity $Z_1=Z_2$, it is not necessary to perform a full skeleton expansion in order to renormalize the charge. In fact, as a consequence of this identity, the photon "charged propagator" (photon full propagator multiplied by the squared bare charge) (see Fig. 10)

$$\begin{aligned} ie_0^2\Delta_{\mu\nu}(p)&=\frac{ie_0^2}{p^2}\left[g_{\mu\nu}-\frac{p_\mu p_\nu}{p^2}\right]+\cdots \\ &\equiv\frac{ie^2(p^2)}{p^2}\left[g_{\mu\nu}-\frac{p_\mu p_\nu}{p^2}\right] \end{aligned} \tag{14}$$

is a finite function by itself [22]. Therefore, in QED, we have the alternative of using the dressed-photon expansion instead of the dressed-vertex expansion. That is, the renormalization-group equation is performed on the photon two-point function [effectively the "running coupling constant" $e(p^2)$] rather than on the fermion-photon-fermion vertex, and all other Green's functions (including the fermion full propagator and the fermion-photon-fermion vertex) are to be expressed in terms of dressed-photon diagrams.

FIG. 10. The photon charged propagator in QED.

FIG. 11. Lowest-order dressed-photon diagram for the computation of the muon anomalous magnetic moment.

This is essentially the basis behind BLM's [4] method of an automatic scale-setting procedure in the case of QED. For instance, the lowest dressed-photon graph for the computation of the muon anomalous magnetic moment is given in Fig. 11. The result from this diagram can be expressed as

$$a_\mu=\frac{\alpha(Q^{*2})}{2\pi}=\frac{e^2(Q^{*2})}{8\pi^2}\ , \tag{15}$$

where Q^* is the effective scale. Notice that the loop integral of this diagram is performed with the running coupling constant (i.e., the photon charged propagator) inside the integrand; therefore, $e^2(Q^{*2})$ effectively is the value obtained though the mean-value theorem by pulling the running coupling constant out of the integral. By using the running coupling constant $e(p^2)$ to one-loop order and neglecting the muon loop effects, this effective scale can be shown to be [23]

$$Q^*=m_\mu\exp(-\tfrac{5}{4})\ . \tag{16}$$

The fermion full propagator (mass and wave-function renormalization effects) is also to be computed with dressed-photon diagrams. The diagrammatic expansion is depicted in Fig. 12, but we shall not get into detailed discussion on this subject here.

The association of charge renormalization to a two-point function rather than a vertex function is not an exclusive property of QED. As we shall see shortly, the leading $1/N$ Gross-Neveu model in the auxiliary field form also exhibits this feature.

Finally, we wish to point out a general misconception about BLM scale-setting method. In QED to the one-loop level, the BLM method is equivalent to the absorption of the light-fermion family number n_f into the running coupling constant. From our point of view, this useful coincidence is peculiar to QED, and should probably not be regarded as the strict definition of the BLM scale-setting method when extending to other field theories [24].

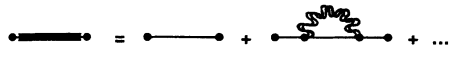

FIG. 12. Full fermion propagator in the dressed-photon expansion.

V. GROSS-NEVEU MODEL IN LEADING $1/N$ EXPANSION

This section is motivated by Stevenson's analysis of the PMS method in the Gross-Neveu model [25]. We shall consider this model with the presence of the auxiliary scalar field σ [3,26]. The Lagrangian density of this model is given by

$$\mathcal{L}=\bar{\Psi}^a(i\partial\!\!\!/)\Psi_a-\tfrac{1}{2}\sigma^2-g_0\bar{\Psi}^a\Psi_a\sigma, \quad a=1,2,\ldots,N \ . \tag{17}$$

The bare propagators and vertex functions of this theory are depicted in Fig. 13 and are given by

$$\begin{aligned} &-i\Delta_0=-i \ , \\ &iD_0{}^a{}_b=\frac{i\delta^a{}_b}{p\!\!\!/+i\varepsilon} \ , \\ &-i\Gamma_0{}^a{}_b=-ig_0\delta^a{}_b \ . \end{aligned} \tag{18}$$

Let us analyze the off-shell fermion four-point function. Although this is not a "physical" quantity in the usual sense (because of its off-shell nature), it nevertheless provides a simple Green's function where various ideas about scale-fixing methods can be tested. For our purpose, we shall only deal with perturbative quantities and bypass all nonperturbative effects arising from dynamical symmetry breaking [28]. The fermion four-point function to leading order in $1/N$ has the structure (Fig. 14)

$$G(p_1,p_2,p_3,p_4)^{ab}{}_{cd}=-ig_0^2[\Delta(s)\delta^a{}_c\,\delta^b{}_d-\Delta(u)\delta^a{}_a\,\delta^b{}_c] \ , \tag{19}$$

where $\Delta(s)$ is the full propagator of the scalar particle to leading order in $1/N$, $s=(p_1+p_3)^2$ and $u=(p_1+p_2)^2$.

Notice that, for the Gross-Neveu model in the auxiliary scalar field context, every vertex in a given Feynman diagram counts as a negative unit power in N, while every scalar propagator represents a positive unit power in N. Thus, in the leading $1/N$ expansion there is no vertex fermion self-energy corrections since these effects are higher order in $1/N$ [26]. Thus, only the full scalar propagator multiplied by the squared bare charge needs renormalization. In the following we shall refer to this function as the "charged scalar propagator." That is, we can choose to "dress up" the charged scalar propagator instead of the three-point vertex function. This resembles the case of QED, where, due to the fact that $Z_1=Z_2$ [4], only the charged photon propagator needs to be renormalized in order to renormalize the bare charge.

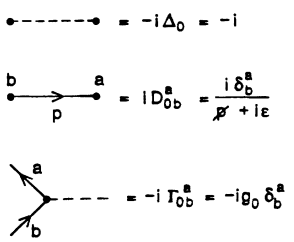

FIG. 13. Bare propagators and coupling vertex of the massless Gross-Neveu model.

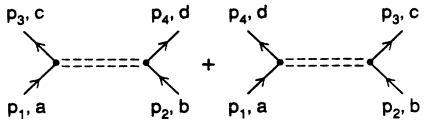

FIG. 14. The fermion four-point function to leading order in $1/N$. The double-dashed line represents the full scalar propagator to leading order in $1/N$.

Naturally one can insist on "dressing up" the three-point function rather than the two-point scalar function. But, as we shall see shortly, both procedures will lead to the same result. Let us consider now the first case. More concretely, let us illustrate the application of the renormalization-group equation (RGE), temporarily up to sixth order in the bare coupling constant.

The charged scalar propagator to sixth order in g_0 is (Fig. 15)

$$\begin{aligned} -ig_0^2\Delta(p^2)&\equiv -ig_{\rm DS}^2(p^2) \\ &=g_0^2(-i)+(-i)[ig_0^2\Pi(p^2)](-i) \\ &\quad +(-i)\{[ig_0^2\Pi(p^2)](-i)\}^2 \\ &=-ig_0^2[1+g_0^2\Pi(p^2)+g_0^4\Pi^2(p^2)] \ , \end{aligned} \tag{20}$$

where the subscript DS stands for dressed skeleton. The vacuum-polarization correction is given by (Fig. 15)

$$ig_0^2\Pi(p^2)=-(ig_0)^2(i)^2N\int\frac{d^dk}{(2\pi)^d}\frac{\mathrm{Tr}[k\!\!\!/(k\!\!\!/+p\!\!\!/)]}{k^2(k+p)^2} \ . \tag{21}$$

A straightforward calculation leads to

$$\begin{aligned} &\Pi(p^2)=-\frac{N}{2\pi}\left[\frac{1}{\hat{\epsilon}}+\ln(-p^2-i\varepsilon)\right] \ , \\ &\frac{1}{\hat{\epsilon}}=\frac{1}{\epsilon}-\ln 4\pi+\gamma_E \ , \end{aligned} \tag{22}$$

where we have used dimensional regularization in $d=2+2\epsilon$. Equation (20) can be rewritten as

$$g_{\rm DS}^2(p^2)=g_0^2+g_0^4\Pi(p^2)+g_0^6\Pi^2(p^2) \ , \tag{23}$$

and, by formally inverting this power series to expand g_0^2

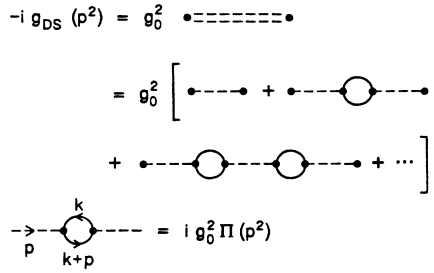

FIG. 15. The charged scalar propagator and the vacuum-polarization diagrams in Gross-Neveu model to leading order in $1/N$.

in power series of $g^2_{DS}(p^2)$,

$$g_0^2 = g^2_{DS}(p^2) - g^4_{DS}\Pi(p^2) + g^6_{DS}(p^2)\Pi^2(p^2) + O(g^8_{DS}) . \tag{24}$$

Now let us obtain the RGE for $g_{DS}(p^2)$. The first step is to differentiate Eq. (23) with respect to the scale variable $x = \ln(-p^2 - i\epsilon)$. Noting that, from Eq. (22),

$$\frac{d\Pi}{dx} = -\frac{N}{2\pi} , \tag{25}$$

we obtain

$$\frac{dg^2_{DS}}{dx} = g_0^4\left[-\frac{N}{2i}\right] + 2g_0^6\Pi(p^2)\left[-\frac{N}{2\pi}\right] . \tag{26}$$

The next step is to replace g_0 by g_{DS} by means of the Eq. (24). After this substitution we obtain a finite RGE for $g^2_{DS}(p^2)$:

$$\frac{dg^2_{DS}}{dx} = -\frac{N}{2\pi}\{[g^2_{DS}(p^2) - g^4_{DS}(p^2)\Pi(p^2) + \cdots]^2 + 2g^6_{DS}(p^2)\Pi(p^2)\} . \tag{27}$$

To order g^6_{DS}, this equation is simply

$$\frac{dg^2_{DS}}{dx} = -\frac{N}{2\pi}g^4_{DS} + O(g^8_{DS}) . \tag{28}$$

Notice that the order-six coefficient has all but vanished. This is a general result for this model: no matter how many terms we start with, all higher-order terms in the RGE (28) will vanish. (This result would be obvious if we had applied the RGE to g^{-2}_{DS} instead of g^2_{DS}, but here we have chosen to present the RGE for g^2_{DS} in order to indicate the procedure for a general field theory.) In other words, we always obtain the exact infinite-order solution:

$$g^2_{DS}(p^2) = \frac{2\pi}{N\ln(-p^2/\Lambda^2_{GN} - i\epsilon)} , \tag{29}$$

independent of the number of terms we have included in the original equation for the charged scalar propagator [Eq. (20)]. This is true even if we have only included the lowest loop correction.

Naturally, we could have chosen to dress up the three-point vertex function rather than the two-point scalar function. But we can see that, in this particular model, these two approaches are completely equivalent. More specifically, to dress up the vertex function we need to obtain first the effective wave-function renormalization constant of the scalar propagator:

$$-i\Delta(p^2) = -i + (-i)[ig_0^2\Pi(p^2)](-i) + \cdots \equiv (-i)Z(p^2) . \tag{30}$$

Noting that there are no fermion self-energy nor vertex corrections, to renormalize the three-point function we simply multiply the bare vertex function by the square root of the effective scalar wave-function renormalization

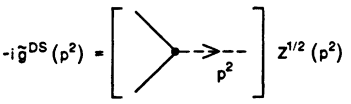

FIG. 16. Dressed three-point function in Gross-Neveu model to leading order in $1/N$.

constant (Fig. 16). Let us designate the renormalized three-point function by $\tilde{g}_{DS}(p^2)$:

$$-i\tilde{g}_{DS}(p^2) \equiv -ig_0 Z^{1/2}(p^2) . \tag{31}$$

But this would imply

$$\tilde{g}^2_{DS}(p^2) = g_0^2 Z(p^2) = g^2_{DS}(p^2) . \tag{32}$$

Thus, dressing up the three-point vertex amounts exactly to dressing up the charged scalar two-point function.

The result for the fermion four-point function is obtained by replacing the Δ function in the Eq. (19) by using

$$g_0^2\Delta(s) = g^2_{DS}(s) = \frac{2\pi}{N\ln(-s/\Lambda^2_{GN} - i\epsilon)} . \tag{33}$$

As shown in Refs. [3] and [25], this is also the exact answer. That is, for the leading $1/N$ massless Gross-Neveu (GN) model, the exact answer is equivalent to the DSE. This should be contrasted with conventional perturbative expansion, where the results are not exact even after applying standard scale-setting methods. In Fig. 17 we plot the symmetrized and the antisymmetrized four-

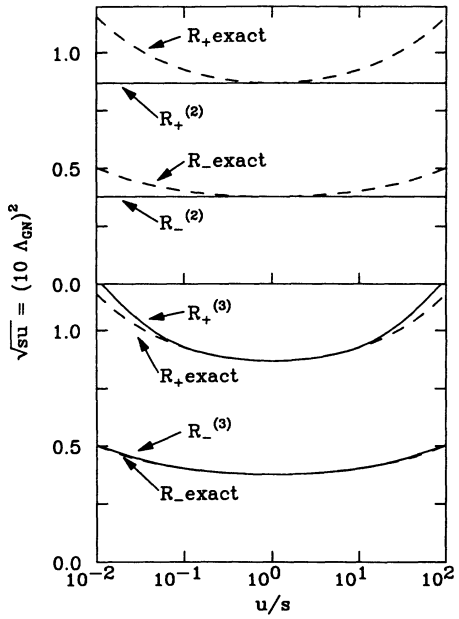

FIG. 17. Symmetrized (R_+) and antisymmetrized (R_-) fermion four-point functions to leading order in $1/N$ in Gross-Neveu model. The dashed lines represent the exact results. The solid lines are the results obtained by applying the PMS optimization method. (a) and (b) correspond, respectively, to the second- and third-order approximant.

point function [27] for spacelike s and u ($s<0$, $u<0$), where the scale has been fixed by applying second- (without scheme variation) and third- (with scheme variation) order PMS scale-scheme setting methods. Following the convention given in Ref. [25], these functions are defined by

$$R_+(s,u)=\frac{g_0^2 N}{2\pi}[\Delta(s)+\Delta(u)]\ ,$$
$$R_-(s,u)=\frac{2g_0^2 N}{\pi \ln(u/s)}[\Delta(s)-\Delta(u)]\ , \tag{34}$$

and are to be calculated in power series of a running coupling constant $g(u^2)$. We do notice from the figure that the third-order approximant improves remarkably over the second-order approximant. This is especially true for the R_- component, which is practically indistinguishable from the exact result in the range plotted. However, these approximants would start to differ from the exact result at higher values of u/s. The conventional scale-setting methods do not give the exact result in this simple model because they assign a single coupling scale to both skeleton graphs. In fact, had the conventional scale-setting procedures (FAC, PMS) been applied to the two skeleton graphs individually, they would have given the exact result, too.

What is the moral of the story? The moral of this exercise is that different skeleton diagrams possess individual renormalization properties, and that by separating different skeleton graphs, at least in this case, one obtains a more exact answer.

VI. $N=2$ GROSS-NEVEU MODEL

In the following we shall consider the $N=2$ Gross-Neveu model without the $1/N$ expansion (this is effectively a two-flavor Thirring model [29,30]). The main purpose of considering this model here is to illustrate the DSE calculation beyond the tree skeleton level. As before, we shall only be interested in performing perturbative calculations, and all nonperturbative effects (dynamical mass generation, spontaneous symmetry breaking [26,29,30], etc.) shall be bypassed. Since the vertex correction is no longer trivial, we cannot choose to dress up the charged two-point function. Instead, we

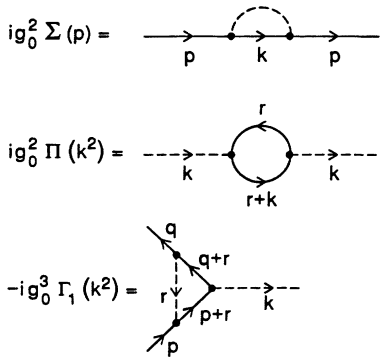

FIG. 18. One-loop, self-energy vacuum-polarization and vertex correction diagrams in the $N=2$ Gross-Neveu model.

should perform the RGE on the three-point vertex function. We shall carry out our calculation within the context of dimensional regularization, with $d=2+2\epsilon$ To one-loop order, the fermion self-energy correction remains zero (see Fig. 18):

$$ig_0^2\Sigma(p)=(-i)(-ig_0)^2\int\frac{d^dk}{(2\pi)^d}\frac{i}{\not k}=0\ . \tag{35}$$

Hence, there is no fermion wave-function renormalization to this order:

$$Z_f(p)=1+O(g_0^4)\ . \tag{36}$$

From the previous section, the scalar propagator for $N=2$ (see Fig. 18)

$$-i\Delta(k^2)=-i+(-i)[ig_0^2\Pi(k^2)](-i)$$
$$=-i\left[1-\frac{g_0^2}{\pi}\left[\frac{1}{\hat\epsilon}+\ln(-k^2-i\varepsilon)\right]\right]\ , \tag{37}$$

from here the effective scalar wave-function renormalization constant is

$$Z_b(k^2)=1-\frac{g_0^2}{\pi}\left[\frac{1}{\hat\epsilon}+\ln(-k^2-i\varepsilon)\right]\ ,$$
$$\frac{1}{\hat\epsilon}=\frac{1}{\epsilon}-\ln 4\pi+\gamma_E\ . \tag{38}$$

The vertex correction (Fig. 18) is given by

$$-ig_0^3\Gamma_1(p,q)=(-i)(-ig_0)^3\int\frac{d^dr}{(2\pi)^d}\frac{i}{\not q+\not r}\frac{i}{\not p+\not r}\ ,$$
$$\Gamma_1(p,q)=\Gamma_1(k^2)=\frac{1}{4\pi}\left[\frac{1}{\hat\epsilon}+\ln(-k^2-i\varepsilon)\right]\ . \tag{39}$$

Combining the self-energy, vacuum-polarization, and vertex corrections, we obtain the renormalized vertex function:

$$-ig_{\rm DS}(k^2)\equiv -ig_0Z_f^{1/2}(q)[1+g_0^2\Gamma_1(k^2)]$$
$$\times Z_f^{1/2}(p)Z_b^{1/2}(k^2)\ . \tag{40}$$

This equation can be put into the form

$$\frac{1}{g_{\rm DS}^2(k^2)}=\frac{1}{g_0^2}+\frac{1}{2\pi}\left[\frac{1}{\hat\epsilon}+\ln(-k^2-i\varepsilon)\right]\ , \tag{41}$$

and its solution is given by

$$g_{\rm DS}^2(k^2)=\frac{2\pi}{\ln(-k^2/\Lambda_{\rm DS}^2-i\varepsilon)}\ . \tag{42}$$

Notice that, if we had used the $1/N$ expansion [compare with Eq. (29)], we would have erred by an overall factor 2. Also notice that the vertex function to this order depends exclusively on the squared momentum of the scalar particle. Now, let us use this vertex function to study the elastic-scattering amplitude of two particles of the same flavor. Consider the process indicated in Fig. 19, where we have chosen the center-of-mass frame to express our kinematics. The corresponding tree skeleton diagrams are indicated in Fig. 20.

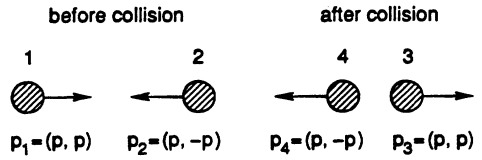

FIG. 19. Kinematics of the elastic collision between two same-flavor particles in the $N=2$ Gross-Neveu model in the center-of-mass frame.

We shall use here $\gamma_0=\sigma_x$ and $\gamma_1=i\sigma_y$. The external fermion wave functions are given by

$$u_1=\sqrt{2p}\begin{bmatrix}1\\0\end{bmatrix},\quad u_2=\sqrt{2p}\begin{bmatrix}0\\1\end{bmatrix},$$
$$\bar{u}_3=\sqrt{2p}\,(0\ 1),\quad \bar{u}_4=\sqrt{2p}\,(1\ 0)\ , \tag{43}$$

and the tree-level amplitude is simply

$$\begin{aligned} iM_{\text{tree}} &= ig_{\text{DS}}^2(t)(\bar{u}_3u_1)(\bar{u}_4u_2)+ig_{\text{DS}}^2(u)(\bar{u}_4u_1)(\bar{u}_3u_2) \\ &= i4p^2g_{\text{DS}}^2(u) \\ &= \frac{i8\pi p^2}{\ln(4p^2/\Lambda_{\text{DS}}^2)}\ . \end{aligned} \tag{44}$$

The Mandelstam variables have the values

$$s=4p^2,\quad t=0,\quad u=-4p^2\ . \tag{45}$$

The one-loop-order skeleton diagram is given in Fig. 21. Let us take some time to discuss these diagrams. First of all, let us compute the box diagrams in the usual perturbation theory, i.e., using the bare coupling constant at the vertices instead of the DS vertex function. By a simple power-counting argument, one can see that the two diagrams are individually ultraviolet divergent. However, it turns out that the divergences coming from the two diagrams cancel each other, as one would expect from the renormalizability of the theory. The Feynman integral of these box diagrams is given by

$$\begin{aligned} iM_{\text{box}} &= g_0^4\int\frac{d^2k}{(2\pi)^2}\left[\bar{u}_3\frac{1}{\not p_1-\not k}u_1\right]\left[\bar{u}_4\frac{1}{\not p_2+\not k}u_2\right] \\ &\quad+\left[\bar{u}_3\frac{1}{\not p_1-\not k}u_1\right]\left[\bar{u}_4\frac{1}{\not p_2-\not k}u_2\right] \\ &= -4p^2g_0^4\int\frac{d^2k}{(2\pi)^2}\frac{k^2}{(k-p_1)^2} \\ &\quad\times\left[\frac{1}{(k+p_2)^2}-\frac{1}{(k-p_2)^2}\right]\ . \end{aligned} \tag{46}$$

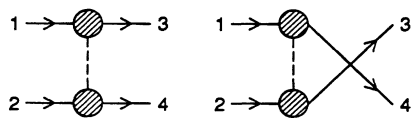

FIG. 20. Tree-skeleton diagrams for two-particle elastic-scattering amplitude in the $N=2$ Gross-Neveu model.

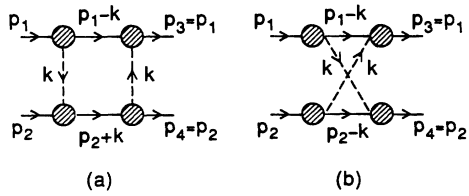

FIG. 21. One-loop skeleton diagram for two-particle elastic-scattering amplitude in the $N=2$ Gross-Neveu model.

The propagators in these expressions come with the $+i\varepsilon$ prescription, and in the language of distribution theory they should be interpreted as the sum of a principal-value part and a δ function:

$$\frac{1}{k^2+i\varepsilon}=P\frac{1}{k^2}-i\pi\delta(k^2)\ , \tag{47}$$

thus the terms in the integrand in Eq. (46) can be classified into the following three types: (1) the product of two principal-value parts; (2) the product of a principal-value part with a δ function; (3) the product of two δ functions.

By direct calculation, it can be shown that the contribution from the first two types of terms vanish; thus, the net contribution of the box diagrams comes entirely from the double δ function terms. In Fig. 22 we plot the location of the singularities of the double δ functions. The result after integration has a simple expression:

$$i\mathcal{M}_{\text{box}}=-p^2g_0^4\ . \tag{48}$$

Now let us return to the dressed skeleton case. We have to replace the bare coupling vertex $-ig_0$ by the dressed-vertex function $-ig_{\text{DS}}(k^2)$. At high energies ($p\gg\Lambda_{\text{DS}}$) the dominant contribution will still be coming from the two double-δ points, the reason for this resides in that these two points are located in deep spacelike and deep timelike regions, i.e., far away from the light cone, and in that $g_{\text{DS}}(k^2)$ is a slow varying function at large $|k^2|$. Therefore, the corrections coming from the infrared be-

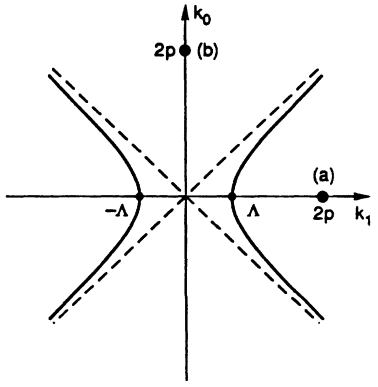

FIG. 22. Location of the double-δ function singularities of the box diagrams (a) and (b) of Fig. 21 in the k_0-k_1 plane. The hyperbola indicates the location of the Landau singularity at $k^2=-\Lambda_{\text{DS}}^2$.

havior of the vertex function $g_{DS}(k^2)$ are expected to be higher twist in nature [31]. In a sense, we can interpret the two points shown in Fig. 22 as the "scale-setting centers" of the skeleton box diagrams. The Landau singularity at $k^2=\Lambda_{DS}^2$ might cause concern about the box integral, but one should bear in mind that this pole is actually located off the real axis due to the presence of the $+i\varepsilon$ term, and as long as we respect this prescription, this pole poses no threat to the finiteness of the box integral. It turns out that box skeleton diagram can be calculated exactly (see the Appendix for the calculation and discussion about the box integral and its renormalons):

$$
\begin{aligned}
i\mathcal{M}_{\text{box}} &= -4p^2 \int \frac{d^2k}{(2\pi)^2} \frac{k^2}{(k-p_1)^2} \\
&\quad \times \left[\frac{1}{(k+p_2)^2} - \frac{1}{(k-p_2)^2} \right] g_{DS}^4(k^2) \\
&= -2p^2 \left[\Psi' \left[\frac{1}{2} - \frac{i}{\pi} \ln(2p/\Lambda_{DS}) \right] \right. \\
&\quad \left. - \Psi' \left[-\frac{i}{\pi} \ln(2p/\Lambda_{DS}) \right] \right] , \qquad (49)
\end{aligned}
$$

where Ψ' is the trigamma function [32]. Needless to say, this amplitude is totally free of scale ambiguity: the result of the skeleton box diagrams is directly expressed in terms of p and Λ_{DS}, and no exogenous coupling has been invoked in the calculation. One can associate an "effective coupling" and an "effective scale" with the box diagram. These functions are defined by [see Eqs. (42) and (48)]

$$
\begin{aligned}
i\mathcal{M}_{\text{box}}(p) &\equiv -p^2 g_{\text{eff}}^4(p) \\
&\equiv p^2 g_{DS}^4(-p_{\text{eff}}^2) \\
&\equiv p^2 \left[\frac{2\pi}{\ln(p_{\text{eff}}^2/\Lambda_{DS}^2)} \right]^2 . \qquad (50)
\end{aligned}
$$

In Fig. 23 we plot the real and imaginary part of the effective coupling constant $g_{\text{eff}}(p)$, and in Fig. 24 we plot the Bode diagrams of amplitude and phase for the effective scale $p_{\text{eff}}(p)$. We observe that, at high energies,

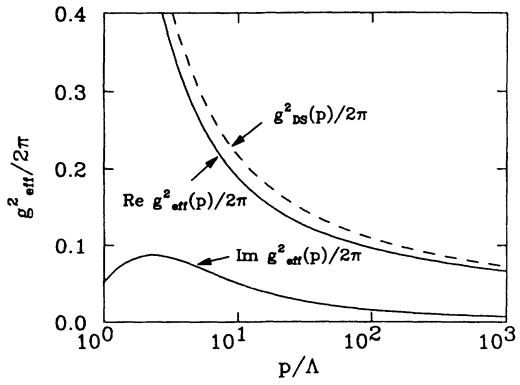

FIG. 23. Real and imaginary parts of the effective coupling constant for the box amplitude of the $N=2$ Gross-Neveu model. Notice that, at high energy $g_{\text{eff}}(p) \to g_{DS}(p)$.

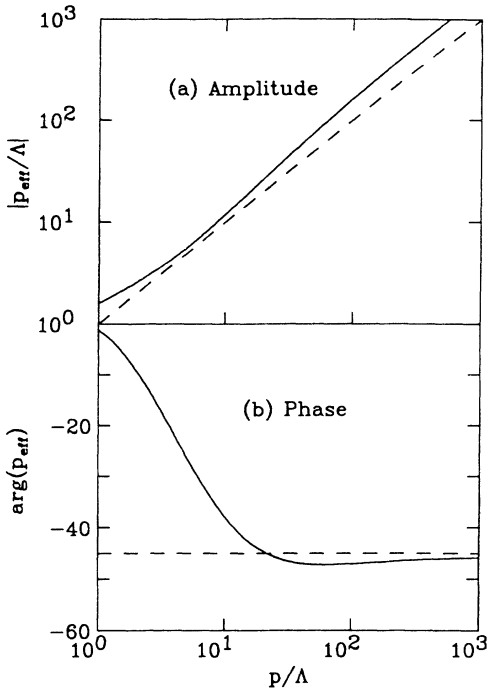

FIG. 24. (a) Bode diagram of amplitude for the effective scale of the box amplitude in the $N=2$ Gross-Neveu model. The dashed line represents $p_{\text{eff}}=p$. (b) Bode diagram of phase (measured in degrees) for the effective scale of the same amplitude. The dashed line indicates $-45°$.

the effective scale has, in the language of phasors, a reactive (negative) angle of 45°. This is expected since one box diagram probes into the deep timelike region while the other box diagram probes into the deep spacelike region (see Fig. 22); thus the effective scale is expected to be half reactive and half resistive. In contrast with conventional scale-setting methods, the effective scales and the effective coupling constants in DSE are, in general, complex numbers.

The total amplitude to one-loop skeleton level is given by the simple addition of the tree-level amplitude [Eq. (44)] and the box amplitude [Eq. (49)]:

$$
i\mathcal{M}_{\text{tot}} = i\mathcal{M}_{\text{tree}} + i\mathcal{M}_{\text{box}} . \qquad (51)
$$

Notice that different order skeletons in general have different effective coupling scales, a feature that has been pointed out in BLM's paper [4].

VII. YUKAWA INTERACTION IN 1+1 DIMENSIONS

The main purpose in using the Yukawa model here is to present the subtleties related to the mass renormalization of propagators and to the matrix structure of vertex functions. While the usage of the skeleton technique for massless scalar bosons is straightforward, the presence of a mass term and the existence of a matrix structure in the various basic vertex functions make the extension of the DSE not immediately trivial. The Yukawa model is chosen because it presents these two features at first-loop level. Although the Yukawa model in 1+1 dimensions is a super-renormalizable theory, this does not affect our

discussion of Dirac structure. The Yukawa theory describes the interaction between a fermion field and a scalar boson field according to the Lagrangian density

$$\mathcal{L}=\bar{\Psi}(i\partial\!\!\!/-m_f)\Psi+\tfrac{1}{2}(\partial^2-m_b^2)\phi^2+\lambda_0 m\bar{\Psi}\Psi\phi\ , \qquad (52)$$

where a mass unit m has been inserted in the interaction term to make the bare coupling λ_0 dimensionless. To simplify our discussion, we shall assume that both the fermion physical mass and the boson physical mass are equal to m. The bare interaction vertex is scalar in the sense that it is given by $-\lambda_0 m$ and thus proportional to the identity matrix (this will be the meaning of the word "scalar" throughout this section). However, this feature is spoiled by the presence of higher-order corrections. The full vertex function will, in general, contain nontrivial Dirac structure:

$$-im\Lambda(p,q)=-im\{\tilde{\Lambda}_0 1+\tilde{\Lambda}_1(p,q)p\!\!\!/+\tilde{\Lambda}_2(p,q)q\!\!\!/ +\tilde{\Lambda}_3(p,q)p\!\!\!/q\!\!\!/\}\ . \qquad (53)$$

In general, the vertex function $\Lambda(p,q)$ will be an N by N matrix, where N is the dimension of the representation of the Dirac algebra, and an immediate question is how to apply the DSE method to obtain all the N^2 components of this vertex function. A first approach would be to write down the RGE's for all the components and solve them separately. But this would introduce N^2 integration constants, that is, N^2 quantities analogous to $\Lambda_{\rm QCD}$. This is hardly necessary, for we know that, aside from the masses of the particles, we only need one more parameter to fix the entire theory. Therefore, we can solve the RGE for only one component, and then expand the other components in terms of the one we have solved for.

The next question is how to choose the component for the RGE. One obvious selection is $\tilde{\Lambda}_0$, for we know that, in the weak-coupling regime, the vertex function should somehow resemble the bare coupling, which is scalar (i.e., proportional to the identity matrix). More precisely, we (1) solve the RGE for $\tilde{\Lambda}_0(p,q)$,

$$\tilde{\Lambda}_0(p,q)=\lambda_0[1+f_1(p,q)\lambda_0^2+f_2(p,q)\lambda_0^4+\cdots]\ , \qquad (54)$$

(2) expand the other components in power series of $\tilde{\Lambda}_0(p,q)$ by inverting Eq. (54). For example, $\tilde{\Lambda}_1$ will have the expression

$$\begin{aligned}\tilde{\Lambda}_1(p,q)&=h_1(p,q)\lambda_0^3+h_2(p,q)\lambda_0^5+\cdots\\&=h_1(p,q)\Lambda_0^3(p,q)\\&\quad+[h_2(p,q)-3f_1(p,q)]\Lambda_0^5(p,q)+\cdots\ .\end{aligned} \qquad (55)$$

While this procedure is formally valid, we shall argue that the four matrices $\{1,p\!\!\!/,q\!\!\!/,p\!\!\!/q\!\!\!/\}$ are not the most desirable choice of basis to decompose Λ. The problem is that when p and q are on shell and the vertex function is multiplied by the external fermion wave functions, the matrices $p\!\!\!/$ and $q\!\!\!/$ can be formally replaced by the scalar matrix $m1$ because the wave functions satisfy the Dirac equation: $(p\!\!\!/-m)u(p)=\bar{u}(q)(q\!\!\!/-m)=0$. This means that, on shell, the matrices $p\!\!\!/$ and $q\!\!\!/$ are indistinguishable from a scalar matrix. Thus, it is highly unnatural to perform the RGE on $\tilde{\Lambda}_0$ for it means that its on-shell value will not be representative of the entire vertex function. Therefore, we are led to the natural choice of basis matrices given by $\{1,p\!\!\!/-m,q\!\!\!/-m,(q\!\!\!/-m)(p\!\!\!/-m)\}$ [33]. Notice that now the nonscalar components $\{p\!\!\!/-m,q\!\!\!/-m,(q\!\!\!/-m)(p\!\!\!/-m)\}$ vanish on shell upon contraction with the external fermion wave functions because of the Dirac equation; thus, the on-shell value of the vertex function is completely contained in the scalar component.

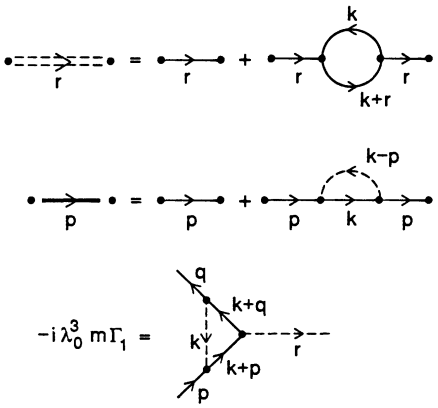

FIG. 25. One-loop scalar and fermion propagator and vertex correction diagrams for the Yukawa model.

Let us carry out the explicit computation of these components of the vertex function in the DSE to one-loop order. The scalar-boson propagator offers no major difficulty: we simply absorb all renormalization effects into the effective wave-function renormalization constant Z_b (Fig. 25):

$$i\Delta_b(p^2)=\frac{i}{p^2-m_b^2}+\frac{i}{p^2-m_b^2}i\lambda_0^2 m^2\Pi(p^2)\frac{i}{p^2-m_b^2}+\cdots\ , \qquad (56)$$

$$i\lambda_0^2 m^2\Pi(r^2)=(-1)(-i\lambda_0 m)^2(i)^2\times\int\frac{d^dk}{(2\pi)^d}\frac{\mathrm{Tr}[(k\!\!\!/+r\!\!\!/+m_f)(k\!\!\!/+m_f)]}{[(k+r)^2-m_f^2](k^2-m_f^2)}\ . \qquad (57)$$

To lowest order, we can replace the bare fermion mass m_f by m in the previous expression, and obtain

$$\Pi(r^2)=-\frac{1}{2\pi}\left[\frac{1}{\hat{\epsilon}}+2+\int_0^1 dx\,\ln[-x(1-x)r^2+m^2-i\varepsilon]\right]\ . \qquad (58)$$

The bare boson mass to order λ_0^2 is given by

$$m_b^2=m^2(1+\lambda_0^2 c_b)\ , \qquad (59)$$

where c_b is the lowest-order counterterm [34]. Replacing (58) and (59) into (56), and retaining only terms to order λ_0^2, we obtain the expression

$$i\Delta_b(r^2)=\frac{i}{r^2-m^2}\left[1+\lambda_0^2 m^2\frac{c_b-\Pi(r^2)}{r^2-m^2}\right] . \quad (60)$$

On mass shell ($r^2=m^2$), Δ_b has a simple pole; therefore, $c_b=\Pi(m^2)$, and

$$i\Delta_b(r^2)=\frac{i}{r^2-m^2}\left[1-\lambda_0^2 m^2\frac{\Pi(r^2)-\Pi(m^2)}{r^2-m^2}\right] \equiv\frac{i}{r^2-m^2}\mathbf{Z}_b(r^2) . \quad (61)$$

The effective wave-function renormalization constant is given by

$$Z_b(r^2)=1-\lambda_0^2 m^2\frac{\Pi(r^2)-\Pi(m^2)}{r^2-m^2} . \quad (62)$$

In particular, the on-shell renormalization constant is

$$Z_{b-\mathrm{OS}}=Z_b(m^2)=1-\lambda_0^2 m^2\left.\frac{d\Pi}{dr^2}\right|_{r^2=m^2} =1-\frac{\lambda_0^2}{2\pi}\left[\frac{2\pi}{3\sqrt{3}}-1\right] . \quad (63)$$

For the fermion propagator we apply a similar procedure (Fig. 25). To one-loop order,

$$i\mathbf{D}_f(p)=\frac{i}{\not p-m_f}+\frac{i}{\not p-m_f}[i\lambda_0^2 m^2\boldsymbol{\Sigma}(p)]\frac{i}{\not p-m_f} , \quad (64)$$

where the self-energy is given by

$$i\lambda_0^2 m^2\boldsymbol{\Sigma}(p)=(-i\lambda_0 m)^2(i)^2\times\int\frac{d^dk}{(2\pi)^d}\frac{\not k+m}{[(k-p)^2-m_b^2](k^2-m_f^2)} . \quad (65)$$

For $\mathbf{D}_f(p)$ to order λ_0^2, we can replace the boson mass m_b by m. After removing the mass counterterm for the fermion mass

$$m_f^2=m^2(1+\lambda_0^2 c_f) , \quad (66)$$

by requiring $\mathbf{D}_f(p)$ to have a simple pole at $p^2=m^2$, we obtain the following expression for the full fermion propagator:

$$i\mathbf{D}_f(p)=\mathbf{Z}_f(p)\frac{i}{\not p-m} ,$$

$$\mathbf{Z}_f^{1/2}(p)=1-\frac{\lambda_0^2}{8\pi}\left[f(p^2)+6\frac{m^2f(p^2)-m^2f(m^2)}{p^2-m^2}\right] -\frac{3\lambda_0^2}{8\pi}\frac{m^2f(p^2)-m^2f(m^2)}{p^2-m^2}\left[\frac{\not p-m}{m}\right] . \quad (67)$$

$$f(p^2)=\frac{m^2}{\sqrt{p^2(p^2-4m^2+i\varepsilon)}}\times\left\{\ln\left[1-\left[\frac{p^2}{p^2-4m^2+i\varepsilon}\right]^{1/2}\right] -\ln\left[1+\left[\frac{p^2}{p^2-4m^2+i\varepsilon}\right]^{1/2}\right]\right\} .$$

Notice that, instead of a scalar wave-function renormalization constant, we have introduced an effective wave-function renormalization matrix. The on-shell expression of this matrix is

$$\mathbf{Z}_{f-\mathrm{OS}}^{1/2}(p)=\mathbf{Z}_f^{1/2}(p)|_{p^2=m^2} =1+\frac{\lambda_0^2}{8\pi}\left[\frac{\pi}{3\sqrt{3}}-4\right] +\frac{\lambda_0^2}{8\pi}\left[\frac{\pi}{3\sqrt{3}}-2\right]\frac{\not p-m}{m} , \quad (68)$$

where the scalar part (the first two terms) is readily identified as the conventional on-shell wave-function renormalization constant. The last term vanishes on shell upon contraction with the associated external fermion wave function.

Let us study the full function at the on-shell boson, one spacelike fermion and one on-shell fermion configuration. That is, $p^2=r^2=m^2$ and $q^2=-Q^2<0$. The vertex function at a completely general momentum configuration could be studied in the same manner, but the expressions involved would be much more complicated.

The vertex correction (Fig. 25) is given by

$$-i\lambda_0^3 m\boldsymbol{\Gamma}_1=(-i\lambda_0 m)^3\int\frac{d^dk}{(2\pi)^d}\frac{(i)^3(\not k+\not q+m)(\not k+\not p+m)}{[(k+q)^2-m^2][(k+p)^2-m^2](k^2-m^2)} , \quad (69)$$

where we have set $m_f=m_b=m$. The decomposition of $\boldsymbol{\Gamma}_1$ into the various components is given by

$$\boldsymbol{\Gamma}_1(q^2)=\frac{1}{4\pi}\left[h_0(q^2)\mathbf{1}+h_1(q^2)\frac{\not p-m}{m}+h_2(q^2)\frac{\not q-m}{Q} +h_3(q^2)\frac{(\not q-m)(\not p-m)}{Qm}\right] \quad (70)$$

with

$$h_0(q^2)=3\int_0^1 dx\int_0^x dy\frac{x-y}{D^2} ,$$

$$h_1(q^2)=\int_0^1 dx\int_0^x dy\frac{1+x-3y}{D^2} ,$$

$$h_2(q^2)=\frac{Q}{m}\int_0^1 dx\int_0^x dy\frac{-1+3x-y}{D^2} , \quad (71)$$

$$h_3(q^2)=\frac{Q}{m}\int_0^1 dx\int_0^x dy\frac{x-y}{D^2} ,$$

$$D=1-y+y^2-(1-x)(x-y)\frac{q^2}{m^2}-i\varepsilon .$$

The renormalized vertex function is given by

$$-im\Lambda(p,q)=-i\lambda_0 m Z_f^{1/2}(q)(1+\lambda_0^2\Gamma_1)Z_{f-\mathrm{OS}}^{1/2}(p)Z_{b-\mathrm{OS}}^{1/2} . \tag{72}$$

Upon decomposition we have

$$\Lambda(p,q)=\lambda_{\mathrm{DS}}(q^2)\mathbf{1}+\lambda_1(q^2)\frac{\not p-m}{m}+\lambda_2(q^2)\frac{\not q-m}{Q} +\lambda_3(q^2)\frac{(\not q-m)(\not p-m)}{Qm} , \tag{73}$$

where we have named the scalar component the dressed skeleton effective coupling constant $\lambda_{\mathrm{DS}}(q^2)$. It satisfies the RGE

$$\frac{1}{\lambda_{\mathrm{DS}}^2(q^2)}=\frac{1}{\lambda_0^2}+\frac{1}{4\pi}\left[f(q^2)-2h_0(q^2) +6\frac{m^2f(q^2)-m^2f(m^2)}{q^2-m^2} +\frac{\pi}{\sqrt{3}}+2\right] \tag{74}$$

with the solution

$$\lambda_{\mathrm{DS}}^2(q^2)=\frac{\lambda^2}{1+(\lambda^2/4\pi)L(q^2)} ,$$
$$L(q^2)=\frac{q^2+5m^2}{q^2-m^2}f(q^2)-2h_0(q^2) -\frac{2\pi}{\sqrt{3}}\frac{m^2}{q^2-m^2}-\frac{2\pi}{3\sqrt{3}}-\frac{7}{2} , \tag{75}$$

where we have chosen the integration constant λ such that $L(q^2=0^-)=0$. That is, λ is the effective coupling at zero spacelike momentum

$$\lambda_{\mathrm{DS}}(q^2=0^-)=\lambda . \tag{76}$$

The general procedure to obtain the other three components involves an expansion of λ_0 in term of $\lambda_{\mathrm{DS}}(q^2)$ by inverting Eq. (74), and then using this substitution in the various $\lambda_i(q^2)$ of Eq. (73). But, to this order, we simply need to replace λ_0 in Eq. (73) by λ_{DS}. The resulting expressions are

$$\lambda_1(q^2)=\frac{\lambda_{\mathrm{DS}}^3(q^2)}{4\pi}\left[h_1(q^2)+\frac{\pi}{6\sqrt{3}}-1\right] ,$$
$$\lambda_2(q^2)=\frac{\lambda_{\mathrm{DS}}^3(q^2)}{4\pi}\left[h_2(q^2)-\frac{3}{2}mQ\frac{f(q^2)-f(m^2)}{q^2-m^2}\right] , \tag{77}$$
$$\lambda_3(q^2)=\frac{\lambda_{\mathrm{DS}}^3(q^2)}{4\pi}h_3(q^2) .$$

In Fig. 26 we plot the different components of the full vertex function for two different values of λ. Notice that, in the weak-coupling regime (say, $\lambda^2/4\pi<0.1$) the renormalization effects become small, namely, the scalar component at high energy only gets slightly renormalized, and the nonscalar ones become comparatively negligible.

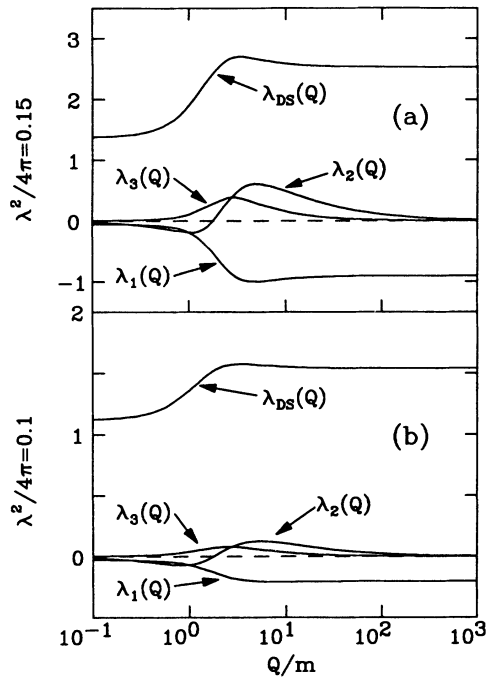

FIG. 26. Different components of the full vertex function of Yukawa model in 1+1 dimensions as obtained by DSE. The external legs of the scalar boson and one of the fermions are on shell; the second fermion has a spacelike momentum $q^2=-Q^2<0$. In (a), $\lambda^2/4\pi=0.15$. In (b), $\lambda^2/4\pi=0.1$.

VIII. SUMMARY AND CONCLUSIONS

We have analyzed the application of the DSE to simple field-theory models in 1+1 dimensions and discussed the various technical features in its implementation. Among the main conclusions we should mention the following.

(1) In the leading $1/N$ Gross-Neveu model, the DSE is equivalent to the exact result. We argue that the trouble of conventional scale-setting methods (FAC, PMS) in yielding the exact result resides in the assignment of a uniform coupling scale to different skeleton graphs.

(2) We have shown in the $N=2$ Gross-Neveu model that loop skeleton diagrams can be meaningfully computed. For asymptotic free theories such as QCD, we indicate that the presence of the Landau singularity at Λ_{QCD} is not expected to pose a threat to loop skeleton integrals, as long as the $+i\varepsilon$ prescription is carefully respected. Also, the effective scale of loop skeleton diagrams is shown to be determined by the kinematics from deep timelike and spacelike regions, thus the detail infrared behavior of the vertex function gives only higher-twist correction. We notice also that the renormalon-type divergences are effectively "packed" into well-defined analytical functions (see the Appendix).

(3) We have extended the DSE to vertex functions involving Dirac matrix structure. For the fermion-boson interaction vertex, we have pointed out that one should

perform the RGE on the scalar component (λ_{DS}) of the vertex function, excluding therefore those components that vanish on shell upon contraction with external fermion wave functions. Once the scalar component is obtained, the nonscalar ones are to be expanded in power series of the scalar component.

The application of the DSE to QCD is discussed in a forthcoming paper.

ACKNOWLEDGMENTS

I thank Professor Stanley Brodsky for the introduction to the scale-setting problem and helpful discussions, and J. D. Bjorken for an enlightening discussion on the development of the skeleton expansion. I also thank Matthias Burkardt, Carl J. C. Im, Carlos A. R. Sá de Melo, Jorge G. Russo, and Brian J. Warr for helpful discussions. This work was supported by the Department of Energy Contract No. DE-AC03-76F00515.

APPENDIX

The skeleton box diagrams indicated in Fig. 21 give the Feynman integral

$$i\mathcal{M}_{\rm box}=-4p^2\int\frac{d^2k}{(2\pi)^2}\frac{k^2}{(k-p_1)^2}\left[\frac{1}{(k+p_2)^2}-\frac{1}{(k-p_2)^2}\right]\times\frac{4\pi^2}{\ln^2(-k^2/\Lambda_{\rm DS}^2-i\varepsilon)}\ . \tag{A1}$$

To perform this integration, let us first expand the inverse square of the logarithm into a power series in $\ln(p^2/\Lambda_{\rm DS}^2)$. Define

$$x=\ln(p^2/\Lambda_{\rm DS}^2),\quad \hat{k}=k/p\ , \tag{A2}$$

we have

$$\ln^{-2}\left[-\frac{k^2}{\Lambda_{\rm DS}^2}-i\varepsilon\right]=\left[\ln\left[\frac{p^2}{\Lambda_{\rm DS}^2}\right]+\ln\left[-\frac{k^2}{p^2}-i\varepsilon\right]\right]^{-2}=[x+\ln(-\hat{k}^2-i\varepsilon)]^{-2}=\frac{1}{x^2}\sum_{n=0}^{\infty}\begin{bmatrix}-2\\ n\end{bmatrix}\frac{\ln^n(-\hat{k}^2-i\varepsilon)}{x^n}\ , \tag{A3}$$

where

$$\begin{bmatrix}-2\\ n\end{bmatrix}=\frac{(-2)(-3)\cdots(-1-n)}{1\times2\times\cdots\times n}=(-1)^n(n+1)\ . \tag{A4}$$

This expansion effectively corresponds to the expansion of the box skeleton diagrams into a power series in the coupling constant at scale p.

By applying the identity

$$\ln^n(-\hat{k}^2-i\varepsilon)=\left[\frac{\partial}{\partial\alpha}\right]^n_{\alpha=0}(-\hat{k}^2-i\varepsilon)^\alpha\ , \tag{A5}$$

the Feynman integrals can be done exactly, the result is

$$i\mathcal{M}_{\rm box}=-\frac{4\pi^2p^2}{x^2}\sum_{n=0}^{\infty}(-1)^n\frac{n+1}{x^n}\left[\frac{\partial f}{\partial\alpha}\right]^n_{\alpha=0}=-\frac{4\pi^2p^2}{x^2}[1-2!f_1x^{-1}+\cdots+(-1)^n(n+1)!f_nx^{-n}+\cdots]\ , \tag{A6}$$

where

$$f(\alpha)=(-4i)^\alpha\sec\left[\frac{\pi\alpha}{2}\right]=f_0+f_1\alpha+f_2\alpha^2+\cdots\ . \tag{A7}$$

We give here the numerical value of the first few coefficients:

$$\begin{aligned}f_0&=1\ ,\\ f_1&=1.38629-i1.5708\ ,\\ f_2&=0.960906-i2.17759\ ,\\ f_3&=0.444033-i2.80132\ ,\\ f_4&=0.15389-i2.48848\ ,\\ f_5&=0.0426674-i2.75823\ ,\\ f_6&=0.00985826-i2.40832\ .\end{aligned} \tag{A8}$$

The expansion (A6) exhibits an $n!$ divergence behavior (because f_i is roughly constant for large value of i), typical of an asymptotic series that needs Borel resummation [9,35] in order to yield a finite result [36]. Fortunately, this series can be Borel resummed exactly, and the result obtained by a straightforward application of the Borel

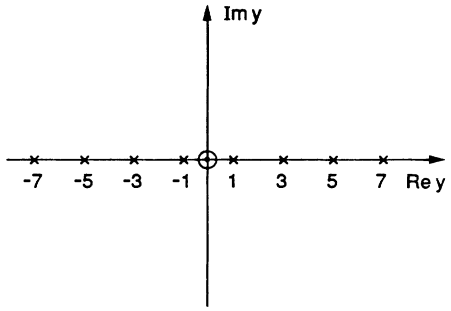

FIG. 27. Location of the singularities of the Borel transform of the box amplitude in the complex-y plane. There is a δ function at the origin and an infinite number of poles located at odd integer numbers, which correspond to renormalon singularities.

resummation formulas is given by

$$i\mathcal{M}_{\text{box}} = -2p^2 \left[\Psi' \left(\frac{1}{2} - \frac{i}{\pi} \ln(2p/\Lambda_{\text{DS}}) \right) - \Psi' \left(-\frac{i}{\pi} \ln(2\pi/\Lambda_{\text{DS}}) \right) \right] , \tag{A9}$$

where Ψ' is the trigamma function [32] defined by

$$\Psi'(z) = \frac{d\Psi}{dz} = \frac{d^2}{dz^2} \ln\Gamma(z) \sim \frac{1}{z} + \frac{1}{2z^2} + \frac{1}{6z^3} - \frac{1}{30z^5} + \frac{1}{42z^7} - \frac{1}{30z^9} + \cdots . \tag{A10}$$

It is interesting to observe that the Borel transform of the series (A6),

$$G(y) \sim \delta(y) + \frac{d^2}{dy^2}[yf(-y)] , \tag{A11}$$

possesses an infinite number of poles on the real axis (see Fig. 27). These poles exhibit the typical feature of renormalon singularities [9,37]. We notice that these poles lie exactly on the real axis; i.e., they do not have an infinitesimal imaginary part. Thus, when performing the Borel integration, those poles on the positive real axis should be interpreted in the principal-value sense. We note that the resulting integral under this prescription is finite, despite the presence of the infinite number of poles.

Notice that if the original integration in Eq. (A1) were performed numerically, we would never have to worry about renormalons. In a sense, the renormalons of this example are effectively absorbed by skeletons.

[1] H. J. Lu and C. A. R. Sá de Melo, Phys. Lett. B **273**, 260 (1991).

[2] M. Korowski, in *The Whys of Subnuclear Physics,* Proceedings of the International School, Erice, Italy, 1977, edited by A. Zichichi, Subnuclear Series Vol. 15 (Plenum, New York, 1979); A. B. Zamolodchikov and A. B. Zamolodchikov, Nucl. Phys. **B133**, 525 (1978); Phys. Lett. **72B**, 481 (1978); Ann. Phys. (N.Y.) **120**, 253 (1979); R. Shankar and E. Witten, Nucl. Phys. **B141**, 349 (1978); B. Berg and P. Weisz, *ibid.* **B146**, 205 (1978); M. Karowski, *ibid.* **B153**, 244 (1979); E. Abdalla, B. Berg, and P. Weisz, *ibid.* **B157**, 387 (1979); M. Karowski and H. J. Thun, *ibid.* **B190**, 61 (1981).

[3] D. J. Gross and A. Neveu, Phys. Rev. D **10**, 3235 (1974).

[4] S. J. Brodsky, G. P. Lepage, and P. B. Mackenzie, Phys. Rev. D **28**, 228 (1983).

[5] G. Grunberg, Phys. Lett. **95B**, 70 (1980); **110B**, 501 (1982); Phys. Rev. D **29**, 2315 (1984).

[6] P. M. Stevenson, Phys. Lett. **100B**, 61 (1981); Phys. Rev. D **23**, 2916 (1981); Nucl. Phys. **B203**, 472 (1982); **B231**, 65 (1984).

[7] A. Dhar, Phys. Lett. **128B**, 407 (1983); A. Dhar and V. Gupta, Pramana **21**, 207 (1983); Phys. Rev. D **29**, 2822 (1984); V. Gupta, D. V. Shirkov, and O. V. Tarasov, Int. J. Mod. Phys. A **6**, 3381 (1991).

[8] The actual implementation of the DSE depends on the specific field-theory model. In general, the renormalization effects of two-point functions can be absorbed into effective wave-function renormalization constants, and the renormalization-group equation is applied directly on the vertex function. However, in some instances, e.g., in QED (where $Z_1 = Z_2$) or in the massless Gross-Neveu model in the leading $1/N$ expansion, one can alternatively choose to dress up the "charged two-point function" instead of the vertex function.

[9] "Renormalons" are singularities in the Borel transform of asymptotic series coming from particular Feynman diagrams. An introduction to the asymptotic nature of perturbative series in quantum field theories and its relation to instantons and renormalons can be found in G. 't Hooft, in *The Whys of Subnuclear Physics* [2].

[10] B. Lautrup, Phys. Lett. **69B**, 109 (1977); P. Olesen, *ibid.* **73B**, 327 (1978).

[11] F. J. Dyson, Phys. Rev. **75**, 1736 (1949).

[12] R. W. Johnson, Ph.D. thesis, Stanford University, 1967.

[13] J. D. Bjorken and S. D. Drell, *Relativistic Quantum Fields* (McGraw-Hill, New York, 1965).

[14] J. Zinn-Justin, *Quantum Field Theory and Critical Phenomena* (Clarendon, Oxford, 1989).

[15] N. N. Bogoliubov and O. S. Parasiuk, Acta. Math. **97**, 227 (1957); K. Hepp, Commun. Math. Phys. **2**, 301 (1966); K. Hepp, *Théorie de la Renormalization* (Springer-Verlag, Berlin, 1969), W. Zimmermann, in *Lectures on Elementary Particles and Quantum Field Theory,* Proceedings of the 1970 Brandeis Summer Institute, edited by S. Deser *et al.* (MIT, Cambridge, Massachusetts, 1970); S. Coleman, in *Properties of the Fundamental Interactions,* edited by A. Zichichi (Editrice Compositori, Bologna, Italy, 1973); J. C. Collins, *Renormalization* (Cambridge University Press, Cambridge, England, 1984); O. I. Zavialov, *Renormalized Quantum Field Theory* (Kluwer Academic, Dordrecht, Netherlands, 1990); V. Rivasseau, *From Perturbative to Constructive Renormalization* (Princeton University, Princeton, NJ, 1991).

[16] N. N. Bogoliubov and D. V. Shirkov, *Introduction to the Theory of Quantized Fields,* 3rd ed. (Wiley, New York, 1980).

[17] O. I. Zav'yalov and B. M. Stepanov, Yad. Fiz. **1**, 922 (1965) [Sov. J. Nucl. Phys. **1**, 658 (1965)]; T. Appelquist, Ann. Phys. (N.Y.) **54**, 27 (1969); S. A. Anikin, O. I. Zav'yalov, and M. K. Polivanov, Theor. Math. Phys. **17**, 1082 (1974); M. C. Bergere and J. B. Zuber, Commun. Math. Phys. **35**, 113 (1974).

[18] M. Baker and C. Lee, Phys. Rev. D **15**, 2201 (1977).

[19] H. Lehmann, K. Symanzik, and W. Zimmermann, Nuovo Cimento **1**, 205 (1955).

[20] T. -P. Cheng and L.-F. Li, *Gauge Theory of Elementary Particle Physics* (Oxford University Press, New York, 1984); C. Itzykson and J. B. Zuber, *An Introduction to Field Theory* (McGraw-Hill, New York, 1980); T. Muta, *Foundations of Quantum Chromodynamics: An Introduction to Perturbative Methods in Gauge Theories* (World Scientific, Singapore, 1987); P. Ramond, *Field Theory: A Modern Primer,* 2nd ed. (Addison-Wesley, New York,

1989); M. Peskin and D. V. Schroeder, *Introduction to Quantum Field Theory* (Addison-Wesley, Massachusetts, 1990).

[21] The skeleton expansion of ϕ_4^4 theory is thoroughly treated by Zinn-Justin, see *Quantum Field Theory and Critical Phenomena* [14].

[22] The Landau gauge has been used here, but in QED we can use any other covariant gauge. It is a well-known fact that the longitudinal part of the photon propagator neither gets renormalized nor contributes to scattering amplitudes. Thus, $e(p^2)$ actually is a gauge-invariant quantity.

[23] There is a numerical mistake in the original BLM paper [4]; the correct answer can be found in J. H. Field, Université de Genève Report No. UGVA-DPNC 1991/3-145 (unpublished).

[24] W. Celmaster and P. M. Stevenson, Phys. Lett. **125B**, 493 (1983); M. R. Pennington, Report No. DTP/83/8 (unpublished); G. Grunberg, Phys. Lett. **135B**, 455 (1984); G. Grunberg and A. L. Kataev, Phys. Lett. B (to be published); G. Grunberg, Phys. Rev. D (to be published).

[25] Application of the PMS scale-scheme setting procedure to the Gross-Neveu model has been studied by P. M. Stevenson, Phys. Rev. D **24**, 1622 (1981).

[26] An elementary introduction to the $1/N$ expansion can be found in S. Coleman, *Aspects of Symmetry* (Cambridge University Press, Cambridge, England, 1985).

[27] We refer the reader to Ref. [25] for the definition and calculation of these quantities. The idea is the four-point function contains a flavor index structure, and the R_+ and R_- functions are, respectively, the symmetric and antisymmetric component of the four-point function under the exchange of flavor indices.

[28] See D. J. Gross and A. Neveu, Phys. Rev. D **10**, 3235 (1974); Coleman, *Aspects of Symmetry* [26]; S. Coleman and E. Weinberg, Phys. Rev. D **7**, 1888 (1973); S. Coleman, *ibid.* **10**, 2491 (1974).

[29] W. E. Thirring, Ann. Phys. (N.Y.) **3**, 91 (1958); Nuovo Cimento **9**, 1007 (1958).

[30] V. Glaser, Nuovo Cimento **9**, 990 (1958); K. Johnson, *ibid.* **20**, 773 (1961); H. Leutwyler, Helv. Phys. Acta **38**, 431 (1965); F. A. Berezin, *The Method of Second Quantization* (Academic, New York, 1966); A. V. Astakhov, O. I. Zav'yalov, and A. D. Sukhanov, Zh. Eksp. Teor. Fiz. **52**, 780 (1967) [Sov. Phys. JETP **25**, 512 (1967)]; G. F. Dell'Antonio, Y. Frishman, and D. Zwanziger, Phys. Rev. D **6**, 988 (1972); A. K. Pogrebkov, Theor. Math. Phys. **17**, 977 (1973); P. de Mottoni, Ann. Inst. Henri Poincaré, Sect. A **16**, 265 (1972). The equivalence between the quantum sine-Gordon model with the massive Thirring model is discussed by S. Coleman, Phys. Rev. D **11**, 2088 (1975); S. Mandelstam, *ibid.* **11**, 3026 (1975); A. Luther, Phys. Rev. B **14**, 2153 (1976).

[31] In Ref. [25] it is pointed out that in the Gross-Neveu case the Landau pole at $k^2=\Lambda_{\rm GN}^2$ is unphysical and that, when the spontaneous symmetry-breaking effects are taken into account, the logarithm that appears in the vertex function should be replaced by

$$B(s,M^2)=\left[\frac{s+4M^2}{2}\right]^{1/2}\ln\left[\frac{(s+4M^2)^{1/2}+\sqrt{s}}{(s+4M^2)^{1/2}-\sqrt{s}}\right], \tag{A12}$$

where M is the dynamically generated fermion mass. This substitution will yield a correction of the order M^2/s, which becomes negligible in the large-s limit.

[32] M. Abramowitz and I. A. Stegun, *Handbook of Mathematical Functions* (Dover, New York, 1972).

[33] This is by no means the unique choice. In fact, any m in this expression can be replaced by a smooth function of p and q, as long as the on-shell value of this function is m. However, we have preferred "static" basis matrices on the ground of simplicity.

[34] Notice that, instead of introducing a mass counterterm interaction in the original Lagrangian, we have preferred to regard the mass in the bare propagator as the bare mass and expand it in terms of the physical mass whenever needed. We have implicitly done the same thing with the coupling constant λ_0 throughout this paper: instead of introducing counterterm vertices, we have preferred to keep the bare coupling bare in our calculation, and expand it in terms of the renormalized coupling whenever needed.

[35] Application of the Borel resummation technique to ϕ^4 field theory in various dimensions can be found in L. N. Lipatov, Pis'ma Zh. Eksp. Theor. Fiz. **25**, 116 (1977) [JETP Lett. **25**, 104 (1977)]; G. 't Hooft, Phys. Lett. **119B**, 369 (1982); J. Zinn-Justin, Phys. Rep. **70**, 109 (1981). Properties of asymptotic series and their resummation techniques can be found in R. B. Dingle, *Asymptotic Expansion, Their Derivation and Interpretation* (Academic, London, 1973).

[36] However, in the large-x limit, this asymptotic series still provides a good approximation to the exact result, as long as we stop summing the series at the term where the series begins to diverge. More precisely, for large x, the first few terms of the series will present an apparent convergence, until the term where $x^n \sim n!$. See Ref. [9] for further discussion on this point and for an elementary introduction to Borel resummation.

[37] G. Parisi, Nucl. Phys. **B150**, 163 (1979); A. H. Mueller, *ibid.* **B250**, 327 (1985).